Air–Fuel Ratio Control of Spark Ignition Engines With Unknown System Dynamics Estimator: Theory and Experiments

Jing Na, *Member, IEEE*, Anthony Siming Chen, Yingbo Huang, Ashwini Agarwal, Andrew Lewis, Guido Herrmann, *Senior Member, IEEE*, Richard Burke, and Chris Brace

***Abstract*— This brief addresses the emission reduction of spark ignition engines by proposing a new control to regulate the air–fuel ratio (AFR) around the ideal value. After revisiting the engine dynamics, the AFR regulation is represented as a tracking control of the injected fuel amount. This allows to take the fuel film dynamics into consideration and simplify the control design. The lumped unknown engine dynamics in the new formulation are online estimated by suggesting a new effective unknown system dynamics estimator. The estimated variable can be superimposed on a commercially configured, well-calibrated gain scheduling like proportional–integral–differential (PID) control to achieve a better AFR response. The salient feature of this proposed control scheme lies in its simplicity and the small number of required measurements, that is, only the air mass flow rate, the pressure and temperature in the intake manifold, and the measured AFR value are used. Practical experiments on a Tata Motors Limited two-cylinder gasoline engine are carried out under a realistic driving cycle. The comparative results show that the proposed control can achieve an improved AFR control response and reduced emissions.**

***Index Terms*— Air–fuel ratio (AFR) control, lambda sensor, spark ignition (SI) engines, unknown dynamics estimator.**

I. Introduction

THE requirement for engine emissions has become more stringent in recent years. To reduce emissions, spark ignition (SI) engines are usually configured with a three-way catalyst (TWC) to convert the pollutant exhaust into innocuous gases [1]. However, it is of great importance that the air–fuel ratio (AFR) in the combustion chamber is maintained at the ideal value because the catalyst conversion efficiency, along with the emissions, heavily depends on the actual AFR value [2]. In fact, the air–fuel mixture in the chamber with the ideal ratio value can deliver optimum thermal efficiency and engine performance [3]. In commercial engine control units (ECUs), one of the widely used AFR control methods is to adjust the injected fuel to fit the intake air mass flow [4].

In general, the AFR control system encounters complicated, nonlinear behavior, when the engine dynamics, model uncertainty, sensor noise, and the fuel puddle dynamics are explicitly considered [5], [6]. Hence, many efforts have been made toward the AFR control design, and different advanced control techniques have been suggested, for example, proportional–integral–differential (PID) control [7], [8], adaptive control [4], [9]–[11], sliding mode control (SMC) [12], [13], and predictive control [14], [15]. Due to its simple structure and parameter tuning phase, PID control with an effective delay compensation was used in [7], and a parameter-varying dynamic compensator was also augmented to a PID control in [8] to address the engine dynamics. However, PID controllers with fixed gains may not be able to account for all nonlinearities effectively over wide operation conditions and then maintain satisfactory AFR response. Thus, an SMC [6] was designed to address the unknown dynamics and maintain fast AFR response. To eliminate the chattering of SMC, a second-order SMC with a neural network was further investigated in [12]. In [13], the effects of time-varying delay, canister purge disturbance, and measurement noise were studied through a second-order SMC. On the other hand, a model predictive control (MPC) was suggested in [14], where a relevance vector machine (RVM) is used to model the AFR loop dynamics. Recently, a model-based predictive control was adopted to improve the in-cylinder AFR response at the lean-burn operation [15]. Other methods such as Fourier analysis [16] and spectral analysis [17] were also explored to deal with the AFR control problem. However, in most of the above AFR control methods, precise engine parameters should be known, or certain internal engine states (e.g., in-cylinder pressure and temperature) should be measured, which cannot be fulfilled in commercial engines, and limit their applicability.

To tackle unknown parameters in the AFR control systems, adaptive control has been used [18]. In [9], a neural network and the corresponding AFR control were synthesized based on the adaptive dynamic programming (ADP). In [11], the biofuel content was online estimated based on the exhaust oxygen AFR sensor signal for a flex fuel lean-burn engine to achieve better AFR response. In [10], an adaptive feedforward control (AFFC) and an adaptive posicast controller (APC) were

Manuscript received April 9, 2019; revised October 16, 2019; accepted October 23, 2019. Manuscript received in final form October 29, 2019. This work was supported in part by the Marie Curie Intra-European Fellowships Project AECE under Grant FP7-PEOPLE-2013-IEF-625531 and in part by the National Nature Science Foundation of China under Grant 61922037 and Grant 61873115. Recommended by Associate Editor M. Tanelli. *(Corresponding author: Jing Na.)*

J. Na and Y. Huang are with the Faculty of Mechanical and Electrical Engineering, Kunming University of Science and Technology, Kunming 650500, China (e-mail: najing25@163.com; yingbo_huang@126.com).

A. S. Chen is with the Department of Mechanical Engineering, University of Bristol, Bristol BS8 1TR, U.K. (e-mail: anthony.chen@bristol.ac.uk).

A. Agarwal, A. Lewis, R. Burke, and C. Brace are with the Department of Mechanical Engineering, Institute for Advanced Automotive Propulsion Systems, University of Bath, Bath BA2 7AY, U.K. (e-mail: a.agarwal@bath.ac.uk; a.g.j.lewis@bath.ac.uk; r.d.burke@bath.ac.uk; c.j.brace@bath.ac.uk).

G. Herrmann was with the Department of Mechanical Engineering, University of Bristol, Bristol BS8 1TR, U.K. He is now with the Department of Electrical and Electronic Engineering, The University of Manchester, Cambridge M13 9PL, U.K.(e-mail: guido.herrmann@manchester.ac.uk).

Color versions of one or more of the figures in this article are available online at http://ieeexplore.ieee.org.

Digital Object Identifier 10.1109/TCST.2019.2951125

proposed to cope with the time delay and the purge fuel disturbance. However, the effect of the inevitable fuel puddle dynamics was not investigated in [9], [10], and [18]. To this end, the model-based adaptive control in [4] considered the fuel film dynamics, where some unknown engine parameters can also be online updated based on the control error signal. Nevertheless, it is known that the transient performance of adaptive methods is heavily related to the learning gains, where the parameter tuning is not a trivial task. Moreover, to implement the adaptive control in [4], extra calculations are required to derive immeasurable engine variables (e.g., fuel mass flow and air mass flow entering the combustion chambers), and a costly torque sensor has to be used because the pumping loss, friction, and load are required in that control implementation.

Viewing the fact that commercial engines usually use well-calibrated PID-based AFR controls, which are easy to understand by engineers, it is desirable to develop AFR control strategies by taking the predefined PID control into consideration and reducing the required measurements. With respect to this motivation, this brief presents a simple yet effective AFR controller using the commonly available engine sensor outputs. We first reformulate the conventional AFR control as an equivalent tracking problem, where the control reference is the corresponding ideal fuel mass flow rate, such that most of the unknown engine dynamics can be merged into a lumped term in the control error dynamics. This allows us to further tailor the unknown system dynamics estimator (USDE) [19], [20] to build a simple, fast, and robust estimator to online reconstruct these lumped unknown dynamics. The estimated variable is then superimposed on a preconfigured, offline calibrated gain scheduling like PID controller as an extra compensation, to achieve a better AFR control response. Consequently, the stringent assumptions on the known engine dynamics and immeasurable variables (e.g., load torque) are avoided. The main contribution of this brief is the new formulation of the AFR control problem and the introduction of the estimator, making the proposed control particularly suited for applications. Compared with the existing SMC and adaptive control schemes [9], [10], [18], the advantages of this proposed AFR control lie in its simplicity, that is, only a constant needs to be set for the estimator, and the reduced requirements on the measurable engine variables. In fact, only the air mass flow, the pressure and temperature in the intake manifold, and the measured AFR value are used, which can be measured through transducers configured in engine products. Finally, when the air mass flow rate into the chamber is not directly measured through sensors in some engines, an online estimation approach is also discussed. The comparative experiments based on a two-cylinder gasoline engine test-rig were carried out, showing improved AFR control response and reduced emissions.

The outline of this brief is as follows. Section II describes the engine dynamics for the control design. Section III presents the typical AFR control framework. Section IV provides the new AFR control framework, control design, stability analysis, and some practical considerations. Section V presents the experimental results and Section VI gives the conclusions.

TABLE I
SPECIFICATION OF ENGINE SYSTEM

Displaced volume	624 cc
Bore / Stroke	73.5 mm * 73.5 mm
Compression ratio	10.3:1
Maximum power	37 bhp @ 5500 RPM
Maximum torque	51 Nm @ 4000 RPM
Firing order	1-2 (360° firing)
Fuel system	Sequential port fuel injection
Emission compliances	Bharat stage (BS) III or IV
Coolant specification	50:50 (water: Ethylene glycol)
Engine management system	Mototune ECU

II. TEST-RIG AND ENGINE DYNAMICS

A. Description of Test-Rig

The experimental work was performed in a bespoke engine test cell at the University of Bath. The main specifications of the engine are given in Table I. The engine was a Tata Motors 273 two-cylinder 624cc gasoline naturally aspirated engine with a bespoke open ECU which allows calibration-level access. In the test-rig, a bespoke interior permanent magnet (IPM) machine and an integrated inverter are directly mounted on the engine crank palm as the engine installation is primarily designed to be used as a range extender. The test cell control system used is CADET V14 from Sierra-CP Engineering enabling monitoring in real-time and logging a range of relevant auxiliary power unit (APU) parameters. A host PC running the CADET V14 software is used to create a virtual instrument for data scaling, processing, and logging. The fuel consumption is measured using a micro motion Coriolis flowmeter. The temperature is measured using chromel–alumel (type-K) mineral insulated thermocouples. Various pressure parameters such as oil pressure, coolant pressure, and fuel pressure are monitored using Druck UNIK 5000 series pressure sensors. The intake air is measured by a Labcell Meriam flowmeter type 50MC2-2F (laminar flow element) equipped with a differential pressure transducer. The mass flow rate is then calculated from the volume flow rate based on the ambient temperature and pressure. The ambient temperature is controlled at 25 °C. The engine management system (EMS) control logic allows for compensation of changes in the ambient temperature and pressure. The engine combustion parameters are measured and logged by an AVL combustion analysis system (CAS).

Undiluted emission concentrations are measured for catalyst gas samples using Horiba MEXA 7000 analyzers. A heated transfer line, at a temperature of 191 °C, is located at the exit of the exhaust ports. The MEXA instrument is calibrated before every experiment using span gases of known concentration and zeroed with nitrogen gas. The universal exhaust gas oxygen (UEGO) sensor is used to measure the real-time AFR value, which is used for the closed-loop fuel control by the engine EMS. (For reasons of brevity, we refer to Section V and [21] for more details on this test-rig.)

B. Engine Dynamics

To facilitate the AFR control system design, we briefly revisit the major engine dynamics to be used, which include the air flow dynamics through the intake manifold and the fuel injection dynamics. The mean-value engine model (MVEM) is used in this brief, where the detailed dynamics have been reported in the literature [5], [22].

1) Throttle Body Dynamics: The air mass flow into the intake manifold is approximated by compressible fluid flow through a converging nozzle. Hence, the mass flow rate $\dot{m}_{ai}$ can be written as

$$\dot{m}_{ai} = m_{at}\frac{p_a}{\sqrt{T_a}} \cdot \mathrm{TC}(\alpha) \cdot \mathrm{PRI}(p_m, p_a) \tag{1}$$

where m_{at} denotes the throttle area, p_a is the ambient pressure, T_a is the ambient temperature, and p_m is the manifold pressure. $TC(\alpha)$ defines the effective throttle area dependent on the plate angle α and the leakage constant α'. $\mathrm{PRI}(p_m, p_a)$ is an influence function defining the compressible flow effects in the throttle [5], [22].

2) Intake Manifold Dynamics: The air-filling dynamics in the manifold determine the air mass flow rate $\dot{m}_{ao}$ entering the chamber, the change in pressure p_m and temperature T_m in the intake manifold with respect to the rotational speed n, and the air mass flow rate $\dot{m}_{ai}$ through the throttle. Hence, the manifold dynamics can be modeled realistically as adiabatic [5], [22], which are given by

$$\dot{p}_m = \frac{\gamma R}{V_i}(\dot{m}_{ai}T_a - \dot{m}_{ao}T_m) \tag{2}$$

$$\dot{T}_m = \frac{RT_m}{p_m V_i}[\dot{m}_{ao}(\gamma - 1)T_m + \dot{m}_{ai}(\gamma T_a - T_m)] \tag{3}$$

where γ is the ratio of heat capacities, R is the ideal gas constant, and V_i is the volume of the intake manifold. Note the above equation describes the variation in pressure p_m and temperature T_m, which is time-dependent [5], [22].

Then, the air mass flow rate entering the chambers can be modeled as

$$\dot{m}_{ao} = \sqrt{\frac{T_m}{T_a}}\frac{V_d\eta_{\mathrm{vol}}}{120RT_m}np_m \tag{4}$$

where V_d is the engine displacement and η_{vol} is the volumetric efficiency [5], [22].

C. Fuelling Dynamics

The fuel injection dynamics determine the actual fuel mass flow rate entering the chamber. Known as the "wall-wetting" phenomenon [4], [5], [22], the fuel flow injected in the manifold is partly deposited on the wall, creating fuel puddles which later enter the cylinder and influence the AFR. The following first-order model can describe the dynamics of fuel puddles:

$$\dot{m}_f = \chi u_f + \dot{m}_{ff}, \quad \kappa\frac{d\dot{m}_{ff}}{dt} = -\dot{m}_{ff} + (1-\chi)u_f \tag{5}$$

where $\dot{m}_f$ is the actual fuel mass flow rate entering the chamber, $\dot{m}_{ff}$ is the fuel flow rate from the liquid fuel films, χ is the portion of the fuel that is delivered instantly into the chamber, κ is the time constant, and u_f is the control command for the injector.

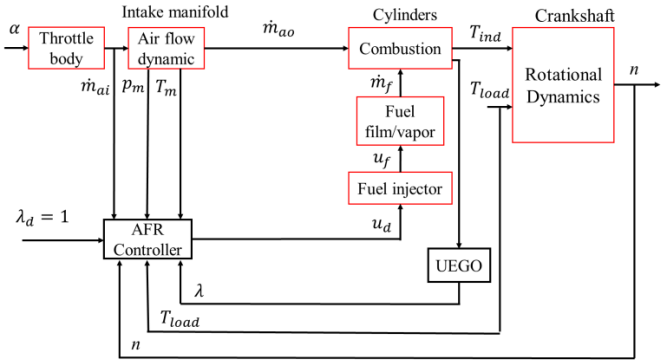

Fig. 1. Block diagram of typical AFR control systems.

Remark 1: In this study, the engine dynamics can be scaled so that the model parameters are with the following units: throttle angle (°), pressure (bar), temperatures (K), engine speed (rpm), torque (N · m), volume (m^3), displacement (L), and mass flow rate (kg/s).

III. Problem Statement

It has been well-recognized that maintaining the desired AFR around the ideal value will help improve the emission performance. The real-time AFR is defined as the ratio of the air flow $\dot{m}_{ao}$ to the fuel flow $\dot{m}_f$, which is given as

$$\lambda = \frac{\dot{m}_{ao}}{\dot{m}_f L_{\mathrm{th}}} \tag{6}$$

where L_{th} is the stoichiometric value ($L_{\mathrm{th}} = 14.12$ in this study). The aim of the AFR control design is to regulate the AFR λ around the ideal AFR value $\lambda_d = 1$. From (6), the AFR λ can be regulated by adjusting the injected fuel mass flow rate $\dot{m}_f$ into the cylinder in correspondence to the air mass flow rate $\dot{m}_{ao}$. This can be achieved by designing the injection control u_f in (5).

In practical AFR control designs, if one uses the dynamics of λ in (6) *directly* as in [4], the full engine dynamics given in (1)–(5) as well as the combustion and crankshaft dynamics will be involved in the derivation of the derivative of λ, making the controller fairly complex and assuming that the essential parameters (e.g., volumetric efficiency, combustion efficiency, and engine torques) should be available/measurable. A typical AFR control system is given in Fig. 1, as used in [4] and [9]–[11].

The inputs of the AFR control system generally include the air mass flow rate $\dot{m}_{ai}$, engine speed n, intake manifold pressure p_m, load torque T_{load}, ideal AFR value $\lambda_d = 1$, and the measured AFR value λ. The output of the AFR control is the required amount of fuel injection command u_d, which is then used to actuate the fuel injector. However, these requirements for the AFR control shown in Fig. 1 may not be fulfilled in commercial engines, that is, the direct measurements of these variables (e.g., torque) or determination of coefficients (e.g., volumetric efficiency) is in general difficult due to the limited sensors and model knowledge. Moreover, the realistic

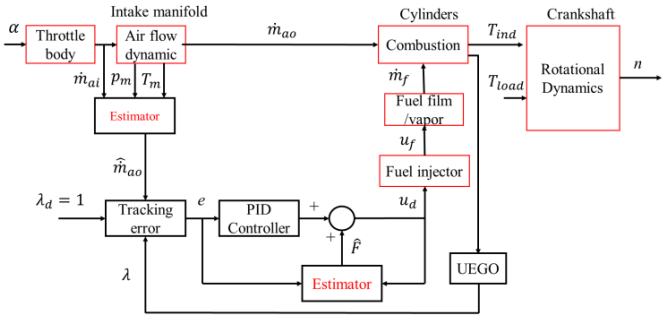

Fig. 2. Block diagram of the proposed AFR controller.

fuel mass flow rate $\dot{m}_f$ and the air mass flow rate $\dot{m}_{ao}$ into the chambers cannot be directly measured, though the real-time AFR λ can be obtained through a UEGO sensor.

Motivations: This brief aims to present an alternative AFR control strategy such that λ can be regulated to as close to the desired value ($\lambda_d = 1$) as possible using limited information (e.g., throttle mass flow rate $\dot{m}_{ai}$, intake manifold pressure p_m, temperature T_m, and the measured AFR λ). The proposed control will remedy the above difficulties stemming from using the dynamics of λ directly as shown in Fig. 1. Moreover, because the commercial ECU usually has a well-calibrated AFR control, for example, gain scheduling like PID control, it is desirable to study simple yet effective control schemes, which can be easily incorporated into a predefined control as shown in this brief.

IV. AFR Control Design With Unknown System Dynamics Estimator

We first reformulate the AFR regulation as an alternative fuel flow rate tracking problem, which allows to estimate the lumped unknown dynamics embedded in the engine dynamics (1)–(5) using a simple USDE. The estimated dynamics are then superimposed on an *a priori* configured AFR feedback control (e.g., a gain scheduling like PID control in our test-rig) as an extra compensator. The new AFR control framework is given in Fig. 2. The tracking error reformulation, the design of the estimator, and the overall control system will be presented.

A. Reformulation of AFR Control Problem

Instead of using the ideal AFR $\lambda_d = 1$ as the control command, we design the AFR control to track the ideal fuel mass flow rate command $\dot{m}_{fd} = (\dot{m}_{ao}/\lambda_d L_{\text{th}})$. Physically, $\dot{m}_{fd}$ defines the reference fuel mass flow required for retaining the ideal AFR λ_d. Hence, the tracking error is defined as the difference between the ideal fuel mass flow rate $\dot{m}_{fd}$ and the actual injected fuel mass flow rate $\dot{m}_f$, which is given by

$$e = \dot{m}_{fd} - \dot{m}_f = \frac{\dot{m}_{ao}}{\lambda_d L_{\text{th}}} - \frac{\dot{m}_{ao}}{\lambda L_{\text{th}}}. \tag{7}$$

It is clear that when the actual fuel mass flow $\dot{m}_f$ entering the chamber is controlled to track the desired reference $\dot{m}_{fd}$, the actual AFR λ can be maintained at the ideal AFR λ_d. The benefit of selecting the mass flow rate $\dot{m}_f$ as the control variable is that the first derivative of error e in (7) with (6) can be calculated using (4) and (5), which is written as

$$\begin{aligned}\dot{e} &= \frac{1}{\lambda_d L_{\text{th}}}\frac{d\dot{m}_{ao}}{dt} - \frac{d\dot{m}_f}{dt} \\ &= \frac{V_d}{\sqrt{T_a}120R\lambda_d L_{\text{th}}}\frac{d(\eta_{\text{vol}} n p_m/\sqrt{T_m})}{dt} + \frac{1}{\kappa}\dot{m}_f - u_d \end{aligned} \tag{8}$$

where u_d represents the control action used to deliver the realistic fuelling command by $u_f = u_d/(\chi s + 1/\kappa)$ as [4].

In (8), the direct calculation of $d(\eta_{\text{vol}} n p_m/\sqrt{T_m})/dt$ requires all engine dynamics given in (1)–(5), where all engine model parameters should be known. However, this calculation is very complicated as the terms $\eta_{\text{vol}}, n, p_m, T_m$ are all time-varying [4]. Fortunately, the reformulated control error allows us to take $d(\eta_{\text{vol}} n p_m/\sqrt{T_m})/dt$ as a part of the lumped unknown dynamics with respect to the tracking error e and control input u_d. Then, we can further tailor the USDE that was newly proposed in [19] and [20] to online estimate these unknown dynamics in (8), and then propose a simple control design without the knowledge of engine model dynamics and tedious calculation of $d(\eta_{\text{vol}} n p_m/\sqrt{T_m})/dt$. Compared with the conventional AFR control given in Fig. 1, the salient feature of this new control framework shown in Fig. 2 lies in that the engine load and speed do not need to be measured.

Remark 2: Even though the actual injected fuel mass flow rate $\dot{m}_f$ may not be measured directly, it is feasible to reformulate the AFR control problem as shown above because the injected fuel $\dot{m}_f$ can be calculated based on (6) using the measurement of real-time AFR λ and the air mass flow rate entering the chamber $\dot{m}_{ao}$.

B. Unknown System Dynamics Estimator

To handle the lumped unknown term in (8), we present a USDE. Then, (8) is rewritten as

$$\dot{e} = F(n, p_m, T_m, \dot{m}_f) - u_d \tag{9}$$

where $F(n, p_m, T_m, \dot{m}_f) = (V_d/\sqrt{T_a}120R\lambda_d L_{\text{th}})(d\left(\eta_{\text{vol}} n p_m/\sqrt{T_m}\right)/dt) + (1/\kappa)\dot{m}_f$ is the lumped unknown dynamics term.

Assumption 1: The unknown term $F(n, p_m, T_m, \dot{m}_f)$ is a continuous function, and its first derivative is bounded, that is, $\sup_{t\geq 0}|\dot{F}| \leq \hbar$ with a positive constant $\hbar$.

The above assumption is practically feasible in the engine application. Hence, to estimate $F(n, p_m, T_m, \dot{m}_f)$, we first define e_f and u_{df} as the filtered variables of e and u_d such that

$$\begin{cases} k\dot{e}_f + e_f = e, & e_f(0) = 0 \\ k\dot{u}_{df} + u_{df} = u_d, & u_{df}(0) = 0 \end{cases} \tag{10}$$

where $k > 0$ is a tuning parameter. It is noted that the variables e_f and u_{df} can be calculated by applying a low-pass filter $1/(ks+1)$ on the measured variables e and u_d.

Hence, the estimator of F can be written as

$$\hat{F} = \frac{e - e_f}{k} + u_{df}. \tag{11}$$

The convergence of the estimation error $e_F = F - \hat{F}$ for estimator (11) can be summarized in the following Lemma.

Lemma 1: For system (9) with estimator (11), then the estimation error e_F is bounded by $|e_F(t)| \leq (e_F^2(0)e^{-t/k} + k^2\hbar^2)^{1/2}$, and thus $\hat{F} \to F$ holds for $k \to 0$ and/or $\hbar \to 0$.

Proof: By applying the filter operation $1/(ks+1)$ on both sides of (9), we can verify that

$$\dot{e}_f = F_f - u_{df} \tag{12}$$

where F_f is the filtered version of the unknown function F given by $k\dot{F}_f + F_f = F$. On the other hand, one can verify from (10) that $\dot{e}_f = (e - e_f)/k$. Hence, it follows that the estimator in (11) is exactly the filtered version of F, that is, $\hat{F} = F_f$. Hence, the estimation error e_F can be given as

$$\dot{e}_F = \dot{F} - \dot{F}_f = -\frac{1}{k}(F - \hat{F}) + \dot{F} = -\frac{1}{k}e_F + \dot{F}. \tag{13}$$

Select a Lyapunov function as $V_e = e_F^2/2$, then its derivative can be obtained along (13) as

$$\dot{V}_e = e_F\dot{e}_F = -\frac{1}{k}e_F^2 + e_F\dot{F} \leq -\frac{1}{k}V_e + \frac{k}{2}\hbar^2. \tag{14}$$

Hence, we can obtain the bound of the estimation error by solving (14) as $V_e(t) \leq e^{-t/k}V_e(0) + k^2\hbar^2/2$, which implies that $|e_F(t)| \leq (e_F^2(0)e^{-t/k} + k^2\hbar^2)^{1/2}$. Hence, it can be shown that $\hat{F} \to F$ holds for $k \to 0$ and/or $\hbar \to 0$. $\diamondsuit$

C. Control Design and Stability Analysis

From Lemma 1, the unknown dynamics $F(n, p_m, T_m, \dot{m}_f)$ including the engine dynamics (1)–(5) are online estimated with exponential convergence. Hence, the estimate $\hat{F}$ can be used in the control design to compensate for the effect of these unknown dynamics, without using the tedious calculation of F and other adaptive techniques as in [4].

In this brief, a gain scheduling like PID control with time-varying gains is configured in the ECU, which has been well-calibrated offline, and is easy to understand by the engineers. Hence, we will use the estimated term $\hat{F}$ in (11) as an extra compensator superimposed on the PID control to design a new AFR control as

$$u_d = u_{\text{PID}} + u_{\text{FF}} = k_p e + k_i \int_0^t e(\tau)d(\tau) + k_d\dot{e} + \hat{F} \tag{15}$$

where $u_{\text{PID}} = k_p e + k_i \int_0^t e(\tau)d(\tau) + k_d\dot{e}$ is the predefined PID feedback controller provided by the commercial ECU, where $k_p > 0, k_i > 0, k_d > 0$ denotes the effect of the proportional, integral, and differential gains, respectively. $u_{\text{FF}} = \hat{F}$ is the extra compensator given in (11).

Remark 3: From (7), the tracking error e in the proposed control can be calculated based on the air mass flow rate $\dot{m}_{ao}$ and the measured AFR λ. In our test-rig, $\dot{m}_{ao}$ can be measured directly. For those engines where $\dot{m}_{ao}$ cannot be measured (due to limited hardware transducers), we will suggest another estimator using the measured variables p_m, T_m, and $\dot{m}_{ai}$, which will be discussed in Section IV-D.

Remark 4: The proposed control in (15) uses a compensation action $u_{FF} = \hat{F}$ from estimator (11) and *directly* superimposes it on a predefined PID control. Most production engines have predefined PID controllers in the EMS. Hence, the proposed control is particularly suited for applications to retain a recent controller and improve the AFR response.

The main theoretical result of this brief is given as follows:

Theorem 1: For the AFR control system provided in Fig. 2, the AFR control (15) with USDE (11) can guarantee exponential convergence of the estimation error e_F and control error e to a small compact set around zero, and the AFR λ is retained around the ideal AFR λ_d.

Proof: We substitute (15) into (9), and then calculate the derivative of the control error as

$$\begin{aligned}\dot{e} &= F - \hat{F} - k_p e - k_i \int_0^t e(\tau)d\tau - k_d\dot{e} \\ &= -k_p e - k_i \int_0^t e(\tau)d\tau - k_d\dot{e} + e_F\end{aligned} \tag{16}$$

which can be rearranged as

$$\dot{e} = \frac{1}{1+k_d}(-k_p e - k_i e_i + e_F) \tag{17}$$

where $e_i = \int_0^t e(\tau)d\tau$. To cope with the integral term e_i, we define the augmented error vector as $E = [e_i, e]^T$ and select an augmented Lyapunov function as $V = (1/2)E^T PE + (1/2)e_F^2$ for a positive symmetric matrix P. Then, (17) can be written as

$$\begin{aligned}\dot{E} &= \begin{bmatrix} 0 & 1 \\ \dfrac{-k_i}{1+k_d} & \dfrac{-k_p}{1+k_d} \end{bmatrix} E + \begin{bmatrix} 0 \\ \dfrac{1}{1+k_d} \end{bmatrix} e_F \\ &= AE + Be_F.\end{aligned} \tag{18}$$

In commercial engines, the preconfigured PID control gains k_p, k_i, k_d are calibrated to retain the stability of the control system, such that the matrix $A(t)$ defined in (18) is bounded and can guarantee that the nominal error system $\dot{E} = A(t)E$ is exponentially stable. Then based on the Lyapunov theory ([23, Th. 4.12]), there exist continuous, bounded, positive definite, symmetric matrices $P(t), Q(t) > 0$ such that $\dot{P} + A^T P + PA = -Q$ holds, and thus $E^T PE$ can be taken as a Lyapunov function for the nominal system. In this case, we calculate the time derivative of the augmented Lyapunov function along (13) and (18) as

$$\begin{aligned}\dot{V} &= \frac{1}{2}E^T P\dot{E} + \frac{1}{2}\dot{E}^T PE + \frac{1}{2}E^T\dot{P}E + e_F\dot{e}_F \\ &= -\frac{1}{2}E^T QE + E^T PBe_F - \frac{1}{k}e_F^2 + e_F\dot{F} \\ &\leq -\frac{1}{2}\left(\lambda_{\min}(Q) - \frac{\eta}{2}\right)\|E\|^2 - \left(\frac{1}{k} - \frac{1+\|PB\|^2}{2\eta}\right)e_F^2 + \frac{\eta\hbar^2}{2} \\ &\leq -aV + \beta\end{aligned} \tag{19}$$

where $\eta > 0$ is a positive constant from the Young's inequality, and $a = \min\{(\lambda_{\min}(Q) - \eta/2)/\lambda_{\max}(P), 2(1/k - (1 + \|PB\|^2)/2\eta)\}$ and $\beta = \eta\hbar^2/2$ are positive constants for appropriately selected parameters $\eta \leq 2\lambda_{\min}(Q), k \leq 2\eta/(1 + \|PB\|^2)$. This implies that $V(t) \leq e^{-at}V(0) + \eta^2\hbar^2/2$, and thus the control errors e and e_i and the estimator error e_F will exponentially converge to a compact small set $\Omega := \{e, e_F | |e| \leq \eta\hbar, |e_i| \leq \eta\hbar, |e_F| \leq \eta\hbar\}$. It is obvious that $\lim_{t\to\infty} e(t) = 0, \lim_{t\to\infty} e_i(t) = 0, \lim_{t\to\infty} e_F(t) = 0$ holds

for $\eta \to 0$ and/or $\hbar \to 0$, for which k is adequately small and/or F is constant, and thus the bound of $|\dot{F}|$ is $\hbar = 0$. Therefore, based on the definition given in (7), the AFR λ is maintained around the ideal AFR value λ_d.

Remark 5: As shown in the above proof, the PID control is used to stabilize the nominal closed-loop control system, that is, the condition $\dot{P} + A^T P + PA = -Q$ is fulfilled [23]. Then, the extra compensator $\hat{F}$ is used to address the unknown dynamics to achieve better control performance. This creates a two-degree-of-freedom control structure [24], that is, the design of the USDE is independent of the PID control, and even in the worst case without the compensator, the controlled system is still stable and provides a good initial performance. Nevertheless, the proposed compensator (11) can be incorporated into other AFR controllers to achieve an enhanced AFR control response, without modifying the preconfigured control strategies.

D. Practical Considerations

1) Measurement of Air Mass Flow Rate: In the proposed control implementation, the air mass flow rate entering the chamber $\dot{m}_{ao}$ is used to calculate the feedback error signal e in (7). In the laboratory test-rig, appropriate sensors can be used to online measure it. In some other engines that do not have such transducers, an online estimator using the measurable engine variables p_m and T_m can be suggested. In fact, the air-filling dynamics (2) indicate that $\dot{m}_{ao}$ can be taken as an unknown variable, and thus allow to use the USDE [19], [20], which is designed as

$$\hat{\dot{m}}_{ao} = \frac{1}{T_m}\left(M_{1f} - \frac{V_i}{\kappa R}\frac{p_m - p_{mf}}{k}\right) \tag{20}$$

where M_{1f} and p_{mf} are the filtered variables of $M_1 = \dot{m}_{ai} T_a$ and p_m given by

$$\begin{cases} k\dot{M}_{1f} + M_{1f} = M_1, & M_{1f}(0) = 0 \\ k\dot{p}_{mf} + p_{mf} = p_m, & p_{mf}(0) = 0 \end{cases} \tag{21}$$

with $k > 0$ being the filter parameter.

Lemma 2: Consider estimator (20) for unknown air mass flow rate $\dot{m}_{ao}$, the estimation error $e_m = \dot{m}_{ao} - \hat{\dot{m}}_{ao}$is bounded by $|e_m(t)| \le (e_m^2(0)e^{-t/k} + k^2\bar{\lambda}^2)^{1/2}$, where $\bar{\lambda}$ is the upper bound of $d\dot{m}_{ao}/dt$, that is, $\sup_{t\ge 0}|d\dot{m}_{ao}/dt| \le \bar{\lambda}$, hence $\hat{\dot{m}}_{ao} \to \dot{m}_{ao}$ holds for $k \to 0$ and/or $\bar{\lambda} \to 0$.

Proof: The proof is similar to Lemma 1. Because fast convergence of this estimator is guaranteed, the control response should not be different to the case with the measured air mass flow rate.

E. Parameter Tuning

The proposed control consists of two components, that is, the predefined PID control and the extra compensator (11) based on the estimator with only a scalar k in (10). Consequently, the parameter tuning of this control is trivial in comparison to other approaches. From the theoretical point of view, the PID control gains should be set to stabilize the control system as explained in Remark 5. In commercial engines, the gain scheduling like PID gains are well-tuned by the manufacturer to retain stability and good basic performance (as for the test-rig we used). For estimator (11), only a scalar k needs to be set by the designers. As it is shown in (10), this constant determines the bandwidth of the low-pass filter $1/(ks + 1)$ imposed on the measured variables e and u_d. Hence, based on Lemma 1, k should be set sufficiently small to retain fast convergence, while a too small k may make the filter and the proposed control sensitive to noise and disturbances. Hence, a tradeoff between the convergence rate and the robustness should be considered to set k.

V. Experimental Results

The engine test-rig described in Section II was used as the experimental platform to validate the efficacy of the proposed AFR control. In this platform, the production engine Bosch Motronic EMS was replaced with a bespoke EMS for which calibration-level access was available [21]. This allows necessary changes to be made on the control strategy in the MATLAB/Simulink environment. Hence, the proposed AFR control is coded using Simulink, which is then compiled and flashed on to the ECU. In the test, a gain scheduling like PID control is predefined during calibration of the engine [21], which stabilizes the AFR control system. Hence, we can take this PID control as the baseline control and carry out tests to show the effect of estimator (11) as the extra compensation. In our experiments, the injected air mass flow rate entering the chamber $\dot{m}_{ao}$ is directly measured using the available sensors, and estimator (20) is not used. Following the guideline, the filter constant of the estimator is set as $k = 0.1$ to tradeoff the robustness against noise and the control responses under different engine operation regimes.

In the tests, the engine speed is controlled through an available speed control. The APU is run on the New European Drive Cycle (NEDC) with the APU speed and power demand based on the requirement to maintain battery state of charge of a battery electric vehicle, which was provided by Tata Motors European Technical Centre. The NEDC cycle along with the APU power and speed demand over the full period of 1180 s is shown in Fig. 3. It is seen that the engine speed varies from 0 to 3500 rpm, where in some particular periods, the engine is switched off (based on the APU power demand and battery state of charge). In the test, the ideal AFR demand from the ECU is always $\lambda_d = 1$.

Fig. 4 shows the comparative responses of the engine with the proposed control and the gain scheduling like baseline PID control for the full period 1180 s. It should be noted that at the moment when the engine is switched off (shown in Fig. 3), the lambda sensor output is meaningless. Hence, the detailed AFR response will be shown later with a reduced time-scale 850–1200 s. Fig. 4(a) provides the recorded injected fuel, throttle angle, and manifold temperature, which illustrate that the engine is operated safely and smoothly with both controls. However, there are minor differences at the time instances when the engine changes its speed, which indicates that PID control has more oscillations than the proposed control. This validates the effectiveness of estimator (11).

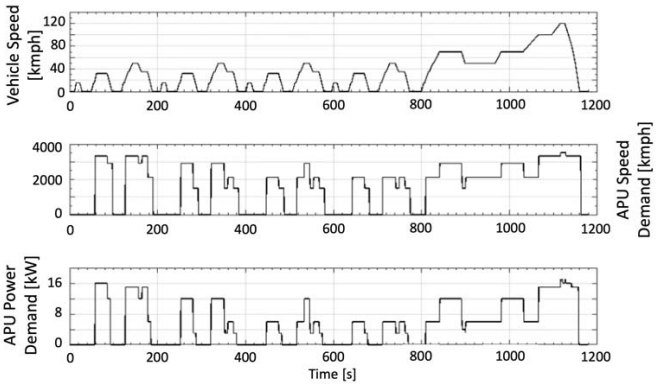

Fig. 3. Full driving cycle used for tests (provided by Tata Motors European Technical Centre).

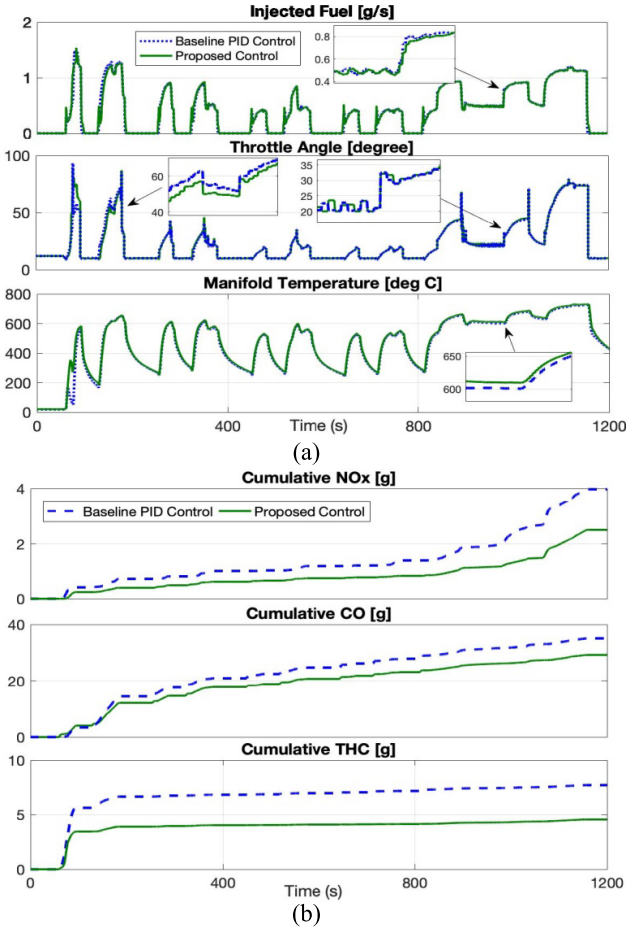

Fig. 4. Experimental results of full drive cycle test. (a) Engine temperature, throttle angle, and injected fuel. (b) Emission responses.

The cumulative emission responses of NOx, CO, and total hydrocarbon emissions (THCs) measured by the configured transducers for full drive cycle are given in Fig. 4(b). From Fig. 4(b), one can find that significantly reduced emissions can be achieved using the proposed control with an extra compensator. In fact, emissions of CO, NOx, and THC vary with different engines, and the AFR of the mixture in the combustion chamber has the greatest influence on the untreated emissions. An engine that is operated at or very close to the ideal AFR enables both NOx reduction (chemically) and CO and HC oxidation in a single catalyst bed. Hence, for a catalyst to be efficient, a very tight control of AFR is necessary, where high conversion efficiencies for all three pollutants can be achieved.

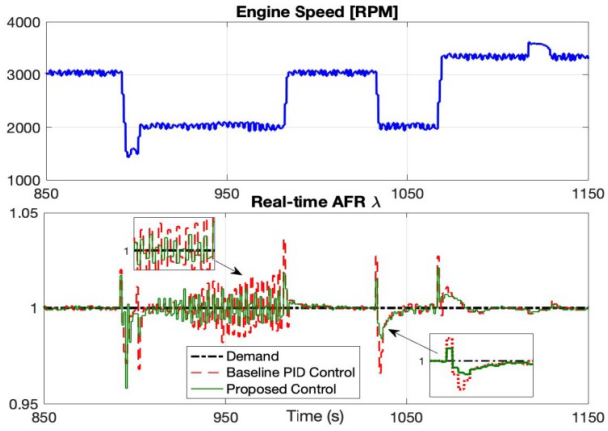

Fig. 5. Engine speed and AFR control response for 850–1150 s.

To show the AFR control response with/without the extra compensator more clearly, we plot the zoomed-in AFR control response from 850 to 1150 s in Fig. 5, when the engine is run with rapidly varying speed (2000 $\sim$ 3200 rpm in the NEDC profile in Fig. 3) but no stops (unlike 0–850 s). This aims to show the efficacy of the proposed estimator and compensator for regulating the AFR value. Compared with the gain scheduling baseline PID control (embedded in bespoke EMS), the suggested estimator and compensation can achieve better AFR control response, that is, it leads to less fluctuations and reduced peak values in the AFR response when the engine changes the speed, showing the benefit of the proposed estimator and compensation. In fact, over 5% improvement (in terms of average value of control error, i.e., $\sum(\lambda - \lambda_d)/T$, for different controllers) has been achieved, which contributes to reduced emissions shown in Fig. 4(b).

Finally, to further show the effectiveness of the proposed control under fast varying engine operation speed, we also carried out dynamic tests, where a manually created engine speed is used as the engine speed control command. As it is shown in Fig. 6(a), the engine speed is controlled to track a square wave command with the period of 80 s and both accelerations and decelerations, that is, $N = 2000 \rightarrow 3500 \rightarrow 2000$ [rpm]. Compared with the NEDC speed profile in Fig. 5, the engine speed in Fig. 6 has faster variations (e.g., the speed increases from 2000 to 3500 rpm during 5 s, and then decreases down to 2000 rpm again within 5 s after 20 s steady-state). This manually created engine speed evolution aims to test the AFR control transient response under fast engine dynamics variations and shows the ability of this proposed control to adapt to these fast variations. The corresponding AFR control responses of the baseline gain scheduling like PID control and the proposed composite control are depicted in Fig. 6(b). One can find from Fig. 6 that the proposed control with the estimator and compensator can again reduce the peak values of the AFR response when the engine changes speed in comparison to the baseline PID control, that is, it achieves a better AFR response.

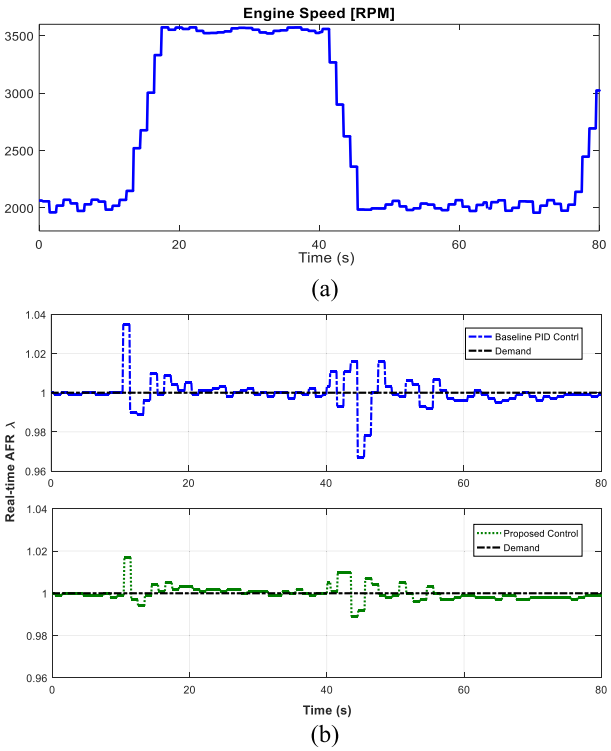

Fig. 6. Comparative AFR control with varying engine speed. (a) Engine speed profile. (b) AFR control responses.

The above experiments with improved AFR responses and reduced emissions all demonstrate the effectiveness and feasibility of the proposed estimator and compensation, which can be easily incorporated into the preconfigured gain scheduling like PID control.

VI. Conclusion

This brief presents a new AFR control framework for SI engines, which is also validated through practical experiments. The main contribution is that the regulation of AFR is reformulated as an equivalent tracking control for the required injected fuel. This allows to use a simple yet effective USDE to address the unknown complex engine dynamics and modeling uncertainty. The estimator output is then added to a predefined AFR control (e.g., gain scheduling like PID control in our test-rig) to obtain a better response. The parameter tuning is straightforward, while better AFR control response and reduced emissions can be achieved compared with the baseline PID control. Another advantage of the proposed control is that it requires the air mass flow, the pressure and temperature in intake manifold, and the real-time AFR only, which can be measured using standard engine sensors. It is noted that the proposed estimator can also be incorporated into other predefined AFR controllers that can stabilize the control system, leading to a two-degree-of-freedom control structure. Practical experiments were conducted on a two-cylinder gasoline engine, which verified the ability of the proposed control to maintain the desired AFR value under different engine running scenarios and reduce engine emissions. Future work will focus on compensating the time-delay effect induced by the sensors to further improve the control response.

References

[1] J. Sun, I. Kolmanovsky, J. A. Cook, and J. H. Buckland, "Modeling and control of automotive powertrain systems: A tutorial," in *Proc. Amer. Control Conf.*, Jun. 2005, pp. 3271–3283.

[2] A. Ghaffari, A. H. Shamekhi, A. Saki, and E. Kamrani, "Adaptive fuzzy control for air-fuel ratio of automobile spark ignition engine," *World Acad. Sci., Eng. Technol.*, vol. 48, pp. 284–292, Dec. 2008.

[3] L. Guzzella and C. Onder, *Introduction to Modeling and Control of Internal Combustion Engine Systems*. Berlin, Germany: Springer, 2009.

[4] X. Jiao, J. Zhang, T. Shen, and J. Kako, "Adaptive air–fuel ratio control scheme and its experimental validations for port-injected spark ignition engines," *Int. J. Adapt. Control Signal Process.*, vol. 29, no. 1, pp. 41–63, 2015.

[5] E. Hendricks and J. Luther, "Model and observer based control of internal combustion engines," in *Proc. Int. Workshop Modelling, Emissions Control Automot. Engines (MECA)*, 2001, pp. 9–20.

[6] S.-B. Choi, M. Won, and J. K. Hedrick, "Fuel-injection control of SI engines," in *Proc. 33rd IEEE Conf. Decision Control*, Dec. 1994, pp. 1609–1614.

[7] E. Franceschi, K. R. Muske, J. C. P. Jones, and I. Makki, "An adaptive delay-compensated PID air fuel ratio controller," SAE Tech. Paper 0148-7191, 2007.

[8] B. Ebrahimi, R. Tafreshi, H. Masudi, M. Franchek, and J. Mohammadpour, "A parameter-varying filtered PID strategy for air-fuel ratio control of spark ignition engines," *Control Eng. Pract.*, vol. 20, no. 8, pp. 805–815, 2012.

[9] D. Liu, H. Javaherian, O. Kovalenko, and T. Huang, "Adaptive critic learning techniques for engine torque and air–fuel ratio control," *IEEE Trans. Syst., Man, Cybern. B. Cybern.*, vol. 38, no. 4, pp. 988–993, Aug. 2008.

[10] Y. Yildiz, A. M. Annaswamy, D. Yanakiev, and I. Kolmanovsky, "Spark ignition engine fuel-to-air ratio control: An adaptive control approach," *Control Eng. Pract.*, vol. 18, pp. 1369–1378, Dec. 2010.

[11] X. Chen, Y. Wang, I. Haskara, and G. Zhu, "Optimal air-to-fuel ratio tracking control with adaptive biofuel content estimation for LNT regeneration," *IEEE Trans. Control Syst. Technol.*, vol. 22, no. 2, pp. 428–439, Mar. 2014.

[12] S. Wang and D. Yu, "A new development of internal combustion engine air-fuel ratio control with second-order sliding mode," *J. Dyn. Syst., Meas., Control*, vol. 129, no. 6, pp. 757–766, 2007.

[13] B. Ebrahimi, R. Tafreshi, J. Mohammadpour, M. Franchek, K. Grigoriadis, and H. Masudi, "Second-order sliding mode strategy for air-fuel ratio control of lean-burn SI engines," *IEEE Trans. Control Syst. Technol.*, vol. 22, no. 4, pp. 1374–1384, Jul. 2014.

[14] H.-C. Wong, P.-K. Wong, and C.-M. Vong, "Model predictive engine air-ratio control using online sequential relevance vector machine," *J. Control Sci. Eng.*, vol. 2012, Jan. 2012, Art. no. 2.

[15] M. Kumar and T. Shen, "In-cylinder pressure-based air-fuel ratio control for lean burn operation mode of SI engines," *Energy*, vol. 120, no. 1, pp. 106–116, Feb. 2017.

[16] W. Schick, C. Onder, and L. Guzzella, "Individual cylinder air–fuel ratio control using Fourier analysis," *IEEE Trans. Control Syst. Technol.*, vol. 19, no. 5, pp. 1204–1213, Sep. 2011.

[17] N. Cavina, E. Corti, and D. Moro, "Closed-loop individual cylinder air–fuel ratio control via UEGO signal spectral analysis," *Control Eng. Pract.*, vol. 18, pp. 1295–1306, Nov. 2010.

[18] C. Khajorntraidet and K. Ito, "Simple adaptive air-fuel ratio control of a port injection SI engine with a cylinder pressure sensor," *Control Theory Technol.*, vol. 13, pp. 141–150, May 2015.

[19] J. Na, A. S. Chen, G. Herrmann, R. Burke, and C. Brace, "Vehicle engine torque estimation via unknown input observer and adaptive parameter estimation," *IEEE Trans. Veh. Technol.*, vol. 67, no. 1, pp. 409–422, Jan. 2018.

[20] J. Na, G. Herrmann, C. Rames, R. Burke, and C. Brace, "Air-fuel-ratio control of engine system with unknown input observer," in *Proc. UKACC 11th Int. Conf. Control (CONTROL)*, Aug./Sep. 2016, pp. 1–6.

[21] A. Agarwal, A. Lewis, S. Akehurst, C. Brace, Y. Gandhi, and G. Kirkpatrick, "Development of a low cost production automotive engine for range extender application for electric vehicles," SAE Tech. Papers 2016-01-1055, 2016.

[22] E. Hendricks and S. C. Sorenson, "Mean value modelling of spark ignition engines," SAE Tech. Paper 900616, 1990.

[23] H. K. Khalil, *Nonlinear Systems*. Upper Saddle River, NJ, USA: Prentice-Hall, 2002.

[24] K. J. Åström and R. M. Murray, *Feedback Systems: An Introduction for Scientists and Engineers*. Princeton, NJ, USA: Princeton Univ. Press, 2010.